A Stereological Analysis of Ductile Fracture by Microvoid Coalescence

JAMES H. STEELE, JR.
Los Alamos National Laboratory, Los Alamos, New Mexico, 87545, USA

ABSTRACT

This analysis for ductile fracture by microvoid coalescence is based upon the three-dimensional model of Widgery and Knott in which microvoids link with a propagating crack if they lie within some interaction distance of its plane. An expression for dimple density is developed from this model using projected image relationships for a thin slab. Void nucleation and growth are incorporated by numerical integration of the Rice-Tracey growth equation for a constant nucleation rate. The stereological approach is evaluated using tensile data for spheroidized 1045 steel to predict the effect of hydrostatic pressure upon damage evolution and dimple density. The analysis provides estimates of dimple size and shape that fit the experimental data, and thus define the parameters that control microvoid coalescence and the micro-roughness of dimpled fracture surfaces.

KEYWORDS

Ductile fracture; Microvoid coalescence; Stereology; Void nucleation and growth; Rice-Tracey growth model; Dimple density.

INTRODUCTION

The ductility and fracture toughness of most engineering alloys that fail by microvoid coalescence (MVC) are controlled by the dispersion of second-phase particles. This is a consequence of the nucleation and growth of microvoids at particles during plastic deformation. These local damage processes, which are statistical in nature, continue until an instability or flow localization process intervenes to produce a macroscopic crack or fracture. The most common instability involves linking of nearest neighbor microvoids by internal necking of the intervening matrix (Thomason, 1968), which localizes plastic deformation to a thin layer that forms the final dimpled fracture surface. Experimental observations clearly show that such MVC is produced by sudden, intense localized necking of the intervoid matrix across a sheet of microvoids, which limits it almost exclusively to a thin layer adjacent to the final fracture surface (LeRoy et al., 1981).

This paper describes a stereological approach based on the geometric model of Widgery and Knott (1978), wherein void coalescence occurs in a thin volume whose thickness represents an interaction distance required for MVC. Internal necking is thus confined to the three-dimensional, continuous, intervoid matrix separating nearest neighbor voids within the volume element defined by the interaction distance. The model defines a unique microstructural size scale for MVC, and thus it may provide the characteristic length needed to relate microstructure and fracture parameters as discussed by Rice (1976). The advantage of this approach lies in the ability to measure the interaction distance and thereby provide a rational basis for evaluating and understanding the critical conditions that control the onset of MVC by internal necking. This paper describes how the geometric model is used to evaluate the physical and microstructural parameters that are involved in the MVC process and in controlling dimple size and shape for uniaxial tensile testing.

STEREOLOGICAL ANALYSIS FOR MICROVOID COALESCENCE

The geometric model of Widgery and Knott, where MVC occurs within in a thin volume of thickness t, furnishes the following projected image relationship (Cahn and Nutting, 1959) between void density, N_V, and expected dimple density, $\langle N_A \rangle$ on the fracture surface:

$$\langle N_A(\text{dimples}) \rangle = N_V(\text{voids}) \{ \langle D_C(\text{voids}) \rangle + t \} \ . \qquad (1)$$

This equation is based upon a thin section through a dispersion of convex microvoids with average caliper diameter $\langle D_C \rangle$, normal to the section, as illustrated in Fig. 1. The model confines the necking instability to the intervoid matrix between nearest neighbors within a planar interaction volume, and thus limits the fracture surface to a statistical sheet of microvoids (Thomason, 1985) as observed (LeRoy et al., 1981). Projected void density at the onset of instability is thus equal to the expected dimple density on the fracture surface, and the intervoid matrix that undergoes necking is defined by Dirichlet cells as shown in Fig. 1b.

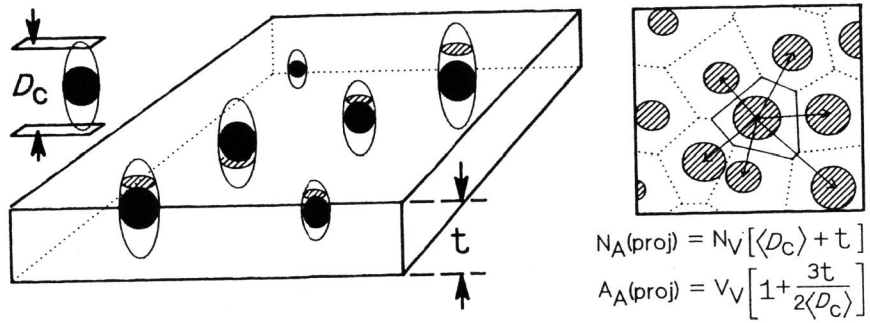

a. thin section b. projected view

Fig. 1 Diagram of thin section through a dispersion of microvoids showing D_C and t and a projected view with nearest neighbors defined by Dirichlet cells and the stereological relationships indicated.

Equation (1) can be expressed in terms of particle density by defining the fraction of particles nucleating voids, $f_n = N_V(v)/N_V(p)$, and a dimensionless thickness, $k = t/\langle D_C(v) \rangle$. Hence dimple density is given as a simple product of physical and microstructural parameters:

$$\langle N_A(\text{dimples}) \rangle = f_n * N_V(p) * \langle D_C(v) \rangle * (k + 1) \ . \qquad (2)$$

The stereological assumptions involved in this relationship are a thin volume sampling of the void dispersion and convex void shapes. The physical conditions implicit in (2) are that necking is confined within the planar volume element; that t is controlled by the critical conditions for instability; and that f_n does not change during MVC. Application of (2) to predict dimple size requires stereological estimates for f_n, $N_V(p)$, $\langle D_C(v) \rangle$, and k, which involve three-dimensional sampling methods (Rhines, 1977). As values for these parameters are not available in studies of ductile fracture, a nucleation and growth model must be used for application of eq. (2).

The most important and most difficult parameter to measure in eq. (2) is the average microvoid size, $\langle D_C(v) \rangle$. This parameter has been employed to describe the critical damage condition for void coalescence (Brown and Embury, 1973). It is also the principal microstructural parameter in local strain models of ductile fracture (Thompson and Ashby, 1984). Evaluation of $\langle D_C(v) \rangle$ requires that void nucleation and growth be either measured or modeled over the strain path for a tensile test. The stereological view is equivalent to the growth path analysis of DeHoff (1971), which requires that void size distributions be measured over the strain path. As void size distributions have not been measured, eq. (2) will be applied using the Rice and Tracey (1969) growth model, and a constant nucleation rate (LeRoy et al. 1981) to describe the void growth paths.

The Rice-Tracey growth model for evolution of noninteracting spherical voids in a remote triaxial stress field has been applied in several studies (Tvergaard and Needleman, 1984, BrownRigg et al., 1983). Principal radii for the axially symmetric ellipsoidal voids that grow under remote tensile stress conditions are given by

$$R3(\varepsilon f, \varepsilon n, \sigma m/\sigma e) = R0 \exp\{ \int_{\varepsilon n}^{\varepsilon f} (\gamma'(\sigma m/\sigma e) + D(\sigma m/\sigma e)) \, d\varepsilon \} \ , \qquad (3)$$

and

$$R1(\varepsilon f, \varepsilon n, \sigma m/\sigma e) = R0 \exp\{ \int_{\varepsilon n}^{\varepsilon f} (-\gamma'(\sigma m/\sigma e)/2 + D(\sigma m/\sigma e)) \, d\varepsilon \} \ , \qquad (4)$$

where R0 = initial void size, εf = fracture strain, εn = nucleation strain, γ' = shape change function, D = dilatational function, and $\sigma m/\sigma e$ = mean stress/effective stress. R3 is the void size in the direction of principal stress and thus, $2R3 = D_C(v)$. R1 is the void size normal to the principal tensile stress. R0 is taken as the size of the nucleating particle, which implies that the physical mechanism for void nucleation is interface decohesion. Also R0 may depend on strain if particle size affects void nucleation. These equations can be used to calculate growth paths for individual voids when the stress state is known as a function of effective plastic strain such as given for tensile tests by BrownRigg et al. Figure 2a shows their equations and a plot of the stress data, which will be used for application. The dilatational function, $D(\varepsilon)$, is given in Fig. 2b along with a plot of its value for the tensile strain path. γ' is taken as approximately 1.67 as indicated by Rice and Tracey (1969) for tensile tests with this range of D.

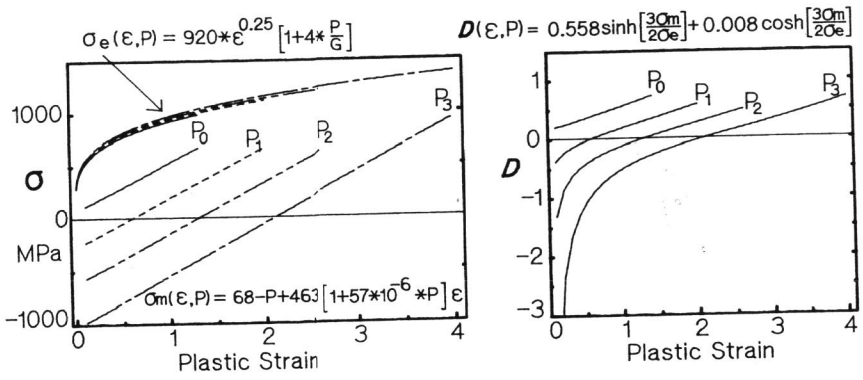

a. Stress functions

b. $D(\varepsilon)$ function

Fig. 2 Stress functions σ_m and σ_e versus plastic strain and $D(\varepsilon)$ for the tensile conditions and pressures P_i from BrownRigg et al. (1983).

Growth paths for voids that nucleate at different plastic strains are readily calculated by numerical integration of (3) and (4) over the strain interval between nucleation and fracture. These results, which are shown in Fig. 3, illustrate the effect of triaxial stress state in increasing void growth rate in the direction of principal stress. They also show that voids tend to contract in the R1 direction rather than grow as suggested by BrownRigg et al. The dependence of R3 on nucleation strain indicates the necessity for establishing an appropriate stereological average of D_C. This is also shown by the data of Argon and Im (1975) where nucleation is dispersed over a significant range of plastic strain.

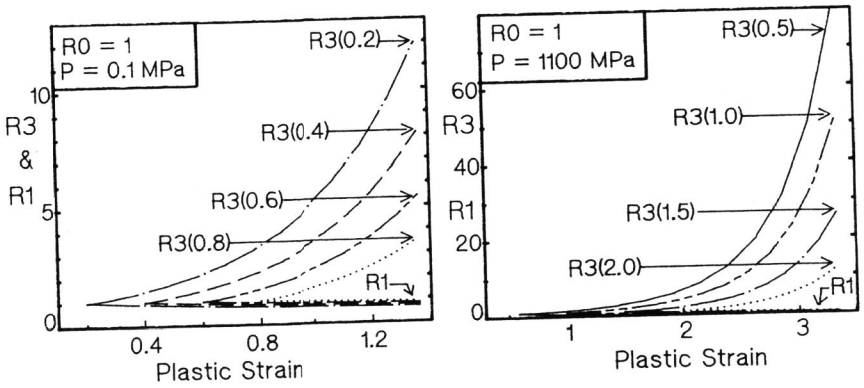

Fig. 3 Growth paths for spherical voids calculated from the Rice-Tracey growth model for varying nucleation strains.

Void nucleation frequency can be expressed as a distribution function normalized over the strain interval for the test

$$F(x) = \int_0^x f(\varepsilon)d\varepsilon = \text{fraction nucleated for } \varepsilon < x \ ,$$

where $f(\varepsilon)d\varepsilon$ is the fraction of voids nucleated in the strain interval to $\varepsilon + d\varepsilon$. The average for D_C is thus given by

$$\langle D_C(\text{voids})\rangle = 2\langle R3\rangle = 2\int_0^{\varepsilon_f} f(\varepsilon)*R3(\varepsilon_f,\varepsilon,\sigma_m/\sigma_e)\ d\varepsilon \ . \qquad (5)$$

The simplest model for $f(\varepsilon)$ is a constant nucleation rate with a starting strain ε_s and ending strain ε_f, as employed by LeRoy et al. (1981) for similar tensile tests. Hence, <R3> is given by

$$\langle R3\rangle = \left\{1/(\varepsilon_f-\varepsilon_s)\right\}\int_{\varepsilon_s}^{\varepsilon_f} R3(\varepsilon_f,\varepsilon,\sigma_m/\sigma_e)\ d\varepsilon \ . \qquad (6)$$

This equation allows <R3> to be calculated by numerical integration using eq. (3). Although other distribution functions could be used for nucleation rate, such as the Gaussian applied by Tvergaard and Needleman (1984), available data are not sufficient to identify the functional form for nucleation frequency.

APPLICATION OF THE MODEL

This section describes the application of the model to experimental data from tensile tests of spheroidized 1045 steel with varying hydrostatic pressure (BrownRigg et al., 1983). Microstructural and test parameters reported for a coarse carbide dispersion are given in Table I.

Table 1. Microstructural and Test Parameters for Spheroidized 1045 Steel tensile tests (BrownRigg et al., 1983).

V_V = 0.066 = Volume fraction of carbides.
<R> = 0.26 μm = Average carbide radius.
<Vol> = 1.1 μm^3 = Average volume selected for nucleation.
N_V = 0.06 μm^{-3} = V_V/<Vol> = Carbides per unit volume.
N_A = 0.03 μm^{-2} = $N_V*\langle D_C\rangle$ = Carbides per unit area.

Pressure (MPa)	ε_s	ε_f	R0 (μm)	f_n	k
0.1	0.30	1.36	0.52	0.50	1.0
345	0.70	1.98	0.55	0.52	1.0
690	1.10	2.60	0.60	0.58	1.0
1100	1.60	3.34	0.63	0.62	1.0

The value for carbide density was selected to be consistent with the largest experimental planar void densities measured. The strain corresponding to the start of nucleation was selected to indicate the beginning of the more profuse nucleation of voids at carbides. Hence, void volume fraction can be calculated using the Rice-Tracey growth model and a constant nucleation rate from

$$V_V(\text{voids}) = N_V(\text{voids})*\langle\text{Volume}\rangle \ , \qquad (7)$$

where $\langle\text{Volume}\rangle = (4\pi/3)*\langle R3\rangle*\langle R1\rangle^2$, since R1 is approximately constant as shown by the growth data in Fig. 3. Calculated void volume fractions

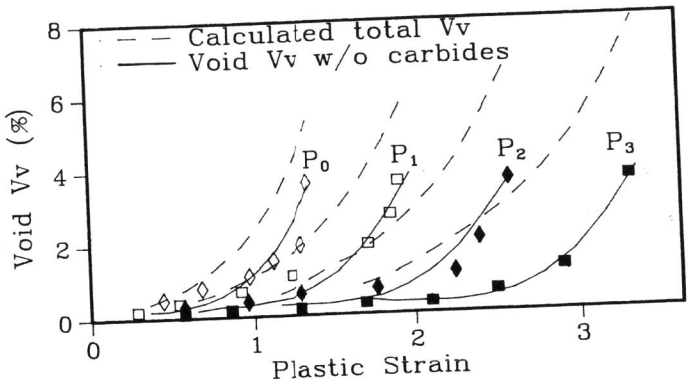

Fig. 4 Plot of calculated void volume fractions and experimental measurements for each test pressure.

are plotted in Fig. 4, along with the experimental volume fraction data. Void volume fractions calculated by subtracting the volume fraction of nucleating carbides show an excellent fit to the experimental data for each hydrostatic pressure. V_V for comparison should not include the nucleating carbides since these were clearly not included in the experimental measurements.

The average value, $\langle D_C(\text{voids})\rangle$, was obtained by numerical integration of eq. (6) for the strain ranges listed in Table I. This allowed the expected dimple density to be estimated for the selected values of f_n and k. f_n, which was not measured by BrownRigg et al., was based upon the experimental data reported by Argon and Im (1975) for 1045 steel with an adjustment to fit the largest experimental V_V levels. The value, k = 1, was selected as a first approximation based upon the model of Brown and Embury (1973) for MVC. The expected dimple density calculated from eq. (2) thus provides an estimate of the average dimple size from

$$D_p = 1.13*(\langle N_A(\text{dimples})\rangle^{-0.5}) \ , \tag{8}$$

which gives the equivalent circle size for the average projected dimple area. Calculated dimple sizes are plotted in Fig. 5 versus hydrostatic pressure for comparison with fractographic measurements. The comparison is excellent even though the measured data were not corrected for a nonplanar fracture surface topography, which may increase their values by 50% (El Soudani, 1974). $\langle R3\rangle$ and $\langle D_p\rangle$ give an estimate of "micro-roughness" (Thompson and Ashby, 1984), $M = \langle R3\rangle/\langle D_p\rangle$. Although experimental measurements are not available for comparison the trend follows that suggested by the highly elongated voids observed with increasing pressure. Calculated values for $\langle R3\rangle$ and M are also shown in Fig. 5 for comparison with the dimple size data. Figure 5 also includes a plot of nearest neighbor spacing within the "interaction volume" calculated from the following equation for a random planar dispersion as in Fig. 1b:

$$\Delta_2 = ((N_A(\text{voids})^{-0.5}) - 2R0 \ . \tag{9}$$

R0 is used in this equation as an estimate for the projected radius of the voids within the interaction volume.

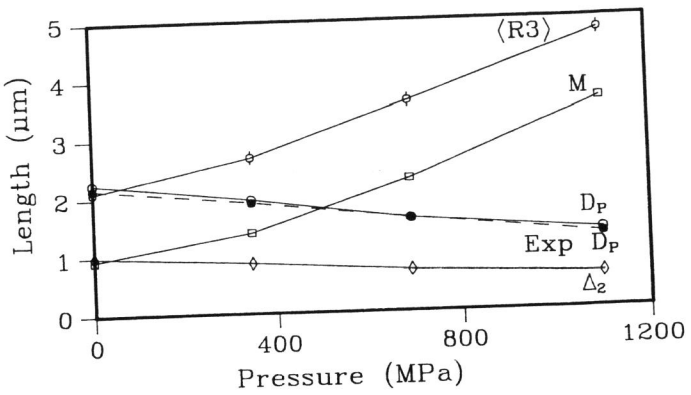

Fig. 5 Plot of calculated dimple size, $\langle R3\rangle$, M, and Δ_2 compared to experimental dimple size data (solid).

DISCUSSION

The results for volume fraction evolution and dimple size variation with pressure indicate that the stereological analysis applied for constant nucleation rate with the Rice-Tracey growth equations provides an excellent description of the MVC process for tensile conditions. The classic overestimate of fracture strain by the Rice-Tracey growth model thus appears to result from the requirement that coalescence occur by lateral void growth rather than the need to incorporate dilatant matrix plasticity. This model is therefore consistent with Thomason's (1985) model that necking instability intervenes to cause MVC before dilatant plasticity of the porous matrix plays any role in the process.

The coalescence model does not specify critical conditions for the necking instability, but rather it indicates how one can evaluate these conditions by applying appropriate stereological section and fractographic measurements. As an example eq. (1) shows that k can be estimated from the dimple density and $\langle N_A(\text{voids})\rangle$ normal to the tensile axis since it can be written as

$$\langle N_A(\text{dimples})\rangle = \langle N_A(\text{voids})\rangle*(k + 1) \ . \tag{10}$$

The value of t can thus be estimated if $\langle D_C(\text{voids})\rangle$ normal to the tensile axis is measured stereologically. This again illustrates the importance of estimating average void size normal to the tensile axis. One method for estimating $\langle D_C(\text{voids})\rangle$ is to assume that the voids are ellipsoids of revolution as in the Rice-Tracey growth model and apply the technique described by DeHoff (1968), which is illustrated in Fig. 6. This method gives $N_V(\text{voids})$, as well as $\langle R1\rangle$ and $\langle R3\rangle$ and thus provides estimates of both nucleation rate and growth paths if applied over the strain path. This result again emphasizes the need to apply appropriate stereological methods for characterizing void nucleation and growth in order to understand ductile fracture and the critical conditions for MVC.

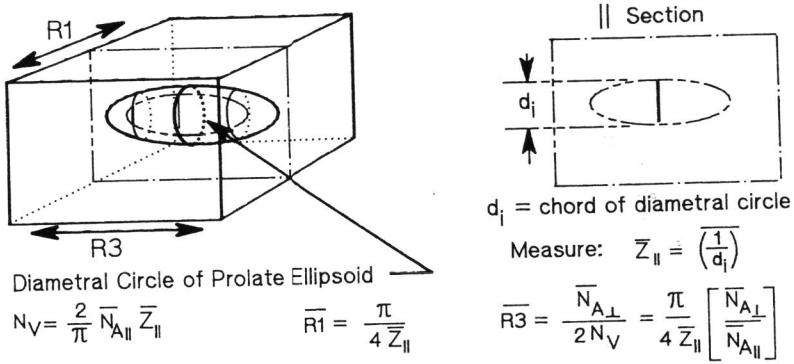

Fig. 6 Stereological analysis for ellipsoidal voids.

REFERENCES

Argon A. S. and J. Im (1975). Separation of second phase particles in spheroidized 1045 steel, Cu-0.6% Cr alloy, and maraging steel in plastic straining. Metall. Trans. A, 6A, 839-851.

Brown L. M. and J. D. Embury (1973). The initiation and growth of voids at second phase particles. In: Proc 3rd Int. Conf. on Strength of Metals and Alloys, Vol. 1, pp. 164-169. Cambridge, England.

BrownRigg A., W. A. Spitzig, O. Richmond, D. Tierlinck and J. D. Embury (1983). The influence of hydrostatic pressure on the flow stress and ductility of a spheroidized 1045 steel. Acta Metall., 31, 1141-1150.

Cahn J. W. and J. Nutting (1959). Quantitative transmission microscopy. Trans. AIME, 215, 526-528.

DeHoff R. T. (1971). The analysis of the evolution of particle size distribution during microstructural change. Metall. Trans., 2, 521-526.

DeHoff R. T. (1968). Measurement of number and average size in volume. In: Quantitative Microscopy(F. N. Rhines and R. T. DeHoff eds.), Chap. 5, pp. 128-148. McGraw-Hill, New York.

El Soudani S. M. (1974). Theoretical basis for the quantitative analysis of fracture surfaces. Metallography, 7, 271-311.

LeRoy G., J. D. Embury, G. Edward, and M. F. Ashby, (1981). A model of ductile fracture based on the nucleation and growth of voids. Acta. Metall., 29, 1509-1522.

Rhines F. N. (1977). Microstructure-Property relationships in materials. Metall. Trans. A, 8A, 127-133.

Rice J. R. (1976). The localization of plastic deformation. In: The Mechanics of Fracture(F. Erdogan, ed.), Vol 19, pp. 23-53. ASME AMD.

Rice J. R. and D. M. Tracey (1969). On the ductile enlargement of voids in triaxial stress fields. J. Mech. Phys. Solids, 17, 201-217.

Thomason P. F. (1968). A theory for ductile fracture by internal necking of cavities. J. Inst. Metals, 96, 360-365.

Thomason P. F. (1985). A three-dimensional model for ductile fracture by growth and coalescence of microvoids. Acta Metall., 33, 1087-1095.

Thompson A. W. and M. F. Ashby (1984). Fracture surface micro-roughness. Scripta Metall., 18, 127-130.

Tvergaard V. and A. Needleman (1984). Analysis of the cup-cone fracture in a round tensile bar. Acta. Metall., 32, 157-169.

Widgery D. J. and J. F. Knott, (1978). Method for quantitative study of inclusions taking part in ductile fracture. Metal Science, 12, 8-11.